European Journal of Radiology 119 (2019) 108639

Contents lists available at ScienceDirect

European Journal of Radiology

journal homepage: www.elsevier.com/locate/ejrad

Research article

Comparison of image quality and radiation doses between rapid kV-switching and dual-source DECT techniques in the chest

Ramandeep Singh, Amita Sharma, Shaunagh McDermott, Fatemeh Homayounieh, Shivam Rastogi, Efren J. Flores, Jo Anne O. Shepard, Matthew D. Gilman, Subba R. Digumarthy*

Department of Radiology, Massachusetts General Hospital and the Harvard Medical School, Boston, MA, USA

ARTICLE INFO

Keywords:
Multidetector computed tomography
Iodine
Artifacts
Dual energy
Chest

ABSTRACT

Purpose: To compare image quality and radiation doses for chest DECT acquired with dual-source and rapid-kV switching techniques.

Materials and methods: Our institutional Review Board approved retrospective study included 97 patients (54 men, 43 women; 63 ± 14 years) who underwent contrast-enhanced chest DECT with both single source, rapid kV-switching (SS-DECT) and dual source (DS-DECT) techniques per standard of care departmental protocols. Reconstructed images from both scanners had identical section thickness and section interval for virtual monoenergetic and material decomposition iodine (MDI) images. Two thoracic radiologists independently evaluated all DECT for findings, quality of images, perfusion defects (MDI), and presence of artifacts. Radiation dose descriptor, size-specific dose estimates (SSDE), was recorded. Data were analyzed with Wilcoxon Signed Rank and Cohen's Kappa tests.

Results: There were no significant differences in patient weight or SSDE for the two DECT techniques ($p > 0.06$). Both radiologists reported no difference in lesion and artifact evaluation on the virtual monoenergetic images from either technique ($p > 0.05$). However, SS-DECT (in 63–71/97 patients) had substantial artifactual heterogeneity in pulmonary perfusion on MDI images compared to none on DS-DECT ($p < 0.001$).

Conclusion: Despite identical patients and associated radiation doses, there were substantial differences in material decomposition iodine images generated from SS-DECT and DS-DECT techniques. Pulmonary heterogeneity on MDI images from SS-DECT leads to artifactual areas of low perfusion and can confound interpretation of true pulmonary perfusion.

1. Introduction

Dual energy CT (DECT) has emerged as a useful scanning technique for evaluation of both vascular and non-vascular thoracic diseases [1–3]. DECT techniques available from various CT vendors deploy substantially different approaches for acquiring DECT data [4].

The dual-source multidetector-row CT scanners (Siemens Healthineers, Forchheim, Germany) acquire DECT or dual-kilovoltage (kV) data from two x-ray tubes which operate simultaneously at different tube potentials in the same gantry rotation. The rapid kV switching DECT technique on single source MDCT scanners (SS-DECT) (GE Healthcare, Milwaukee, WI) switches tube potentials of 80 and 140 kV every 0.25-millisecond as it rotates around the patient. The dual layer detector CT scanner (Philips Healthcare, Eindhoven, The Netherlands) uses a single x-ray source and single tube potential (120 or 140 kV) to parse low and high energy spectra x-rays for generating DECT data. Other DECT data acquisition approaches include single-source twin-beam (Siemens Healthineers, Forchheim, Germany) and single-source separate (spin) rotations (Toshiba, Tochigi, Japan).

Despite major differences between the acquisition approaches of CT vendors, they produce similar image types for virtual monochromatic and material decomposition- iodine (MDI) images.

However, effect of the differences in DECT acquisition techniques on the image quality, lesion appearance, and radiation doses is not well

Abbreviations: CT, computed tomography; DECT, dual energy computed tomography; SS-DECT, single source dual energy computed tomography; DS-DECT, dual source dual energy computed tomography; MDI, material decomposition iodine; SSDE, size specific dose estimates; IRB, institutional review board; HIPAA, health insurance portability and accountability act; PACS, picture archiving and communication system; IQR, interquartile range; WED, water equivalent diameter; ECG, electrocardiogram

* Corresponding author at: Department of Radiology, Massachusetts General Hospital, 202 Founders, 55 Fruit Street, Boston, MA, 02114, USA.
E-mail address: sdigumarthy@mgh.harvard.edu (S.R. Digumarthy).

https://doi.org/10.1016/j.ejrad.2019.08.008
Received 1 March 2019; Received in revised form 7 August 2019; Accepted 9 August 2019
0720-048X/

understood. Prior phantom studies have compared DECT images from different CT vendors but to our knowledge at the time of preparing this manuscript there were no published patient studies on this matter [5–8]. Such evaluation is critical for institutions such as ours which have DECT-capable scanners from more than one CT vendor such as the third-generation dual source CT (DS-DECT) (Somatom Force, Siemens Healthineers) and the single-source rapid kV switching CT (SS-DECT) (Revolution CT, GE Healthcare). The purpose of our study was to assess image quality for virtual monochromatic and material decomposition-iodine images and radiation doses for chest DECT acquired with dual-source and rapid-kV switching techniques.

2. Materials and methods

The institutional review board (IRB) approved our retrospective human subject study with waiver of informed consent from the study subjects. The study was compliant with the Health Insurance Portability and Accountability Act (HIPAA). None of the coauthors have any financial disclosures.

2.1. Patients and scanners

From the Radiology Information System and Picture Archiving and Communication System (PACS; Agfa IMPAX-version 6.6.1.3004, Agfa-Gevaert Group, Mortsel, Belgium), we identified all patients who underwent 15,177 chest CT examinations on either the 192-slice, third-generation dual source (Somatom Force, Siemens Healthineers, Forchheim, Germany; n = 8203 CT exams) or the 256-slice, single-source rapid kV switching (GE Revolution, GE Healthcare, Waukesha, Wisconsin, USA; n = 6974 CT exams) CT scanners between April 2016 and May 2018. Of these, 130 patients underwent chest CT on both scanners. A study co-investigator (RS, 5-year post-radiology residency) reviewed the radiology report and the CT images of these 130 patients to exclude 30 patients who had non-contrast CT, non-chest CT protocol (for thoracic aorta or contiguous single-series chest-abdomen CT), motion and metallic implant-related artifacts, arms by the side. Since the radiation dose parameters such as size specific dose estimates (SSDE) are function of $CTDI_{vol}$ and patient body weight, in order to match our study groups, we excluded patients with significant weight change between the two scans. Three patients had weight change greater than 20% between the two chest CT examinations. These three excluded patients with > 20% weight change between the two CT examinations were used to train the test radiologists for subjective image quality assessment. These cases were not included in the statistical analyses of the study. The final study sample size comprised 97 adult patients (54 men and 43 women; mean age 63 ± 14 years; age range 20–86 years) who had contrast enhanced DECT on both scanners. All examinations were performed for clinically indicated reasons; the most frequent clinical indications were lung cancer, chest pain, hypoxia, and suspected or known complicated pneumonia.

Patient weights were recorded at the time of each CT examination. We also recorded patient's age and gender. The median time interval between the SS-DECT and DS-DECT scans was 157 days (IQR = 60–360 days).

2.2. Scan protocols and image processing

All 97 patients underwent contrast-enhanced chest DECT with 80 mL of intravenous contrast injected at 2–3 mL/second (Iopamidol 370 mg%, Isovue 370, Bracco Diagnostics, Princeton, NJ) on both CT scanners. The DS-DECT examinations were performed at 80 and 150 kV with tin filter at quality reference mAs of 180 mAs using automatic exposure control (Care Dose 4D, Siemens) for the 80-kV x-ray source, 2*2*96*0.6 mm detector configuration with double z-sampling, helical scan mode, 0.9:1 beam pitch, and 0.5 s rotation time. The SS-DECT exams were performed with 80 and 140 kV, noise index of 13–14, 128 x 0.625 mm detector configuration, helical scan mode, 0.992:1 beam pitch and 0.5-0.7 s rotation time. Unlike the combined angular and longitudinal automatic exposure control technique used for DS-DECT, the noise index on the SS-DECT exams helps in selection of fixed tube current values based on the patient size and attenuation but does not modulate tube current in angular or longitudinal directions. We applied the commercial iterative reconstruction techniques to reconstruct images from both scanners – ASiR-V at 40% strength for SS-DECT and ADMIRE at strength of 2 for the DS-DECT. These levels of iterative reconstructions are used for clinical interpretation in our institution. We do not generate any filtered back projection images for these examinations in our practice. Per the institutional standard of care, we generated transverse virtual monoenergetic images at 60 keV and MDI images with 2.5 mm section thickness and 2.5 mm section interval for all DECT examinations on both scanner types. The virtual monoenergetic images are reconstructed at 60 keV per standard of care practice in our Division of Thoracic Imaging for routine thoracic DECT examinations. Since DS-DECT does not directly generate 2.5 mm sections and SS-DECT does not allow reconstruction of 2 or 3 mm section thickness, we reconstructed 2.5 mm section thickness for SS-DECT and reformatted average intensity weighted images at 2.5 mm section thickness for DS-DECT.

2.3. Qualitative evaluation

Two board-certified and fellowship-trained thoracic subspecialty radiologists (with > 5 years of subspecialty experience in interpretation of DECT) independently assessed all 194 DECT examinations from 97 patients on the PACS workstation per the standard of care in our institution. Each radiologist reviewed the DECT examinations in random order so that SS-DECT and DS-DECT were reviewed first with equal frequency. Given the experience of the radiologists and their familiarity with the image appearance from each vendor and differential appearance of images from the two vendors it was not possible to perform a blinded evaluation. Each radiologist assessed transverse 60 KeV virtual monoenergetic and MDI images for qualitative parameters for each scanner. The monoenergetic images were reviewed in both lung (1500 window width, -600 window level) and soft tissue (350 window width, 60 window level) windows, but the radiologists could adjust the window settings per their preference for all viewed image series. Radiologists could review the MDI images of SS-DECT in gray scale or apply color preset (hot preset) as per their preferred standard of care practice. The DS-DECT MDI images were created with color display as per the standard of care setting for that scanner.

Both radiologists reviewed the monoenergetic 60 keV transverse images for each DECT examination separately for any abnormalities of the lungs, pleura, pulmonary arteries, mediastinum, heart and pericardium, and the thyroid gland. They also performed qualitative assessment of overall diagnostic quality, noise texture, as well as artifact types (motion/blur, contrast streaking, beam hardening, metallic implant related artifacts) and their severity. Diagnostic quality was graded on a 4-point scale (1 = non-diagnostic quality due to any reason other than poor contrast enhancement, 2 = suboptimal or limited diagnostic quality; 3 = acceptable or optimal diagnostic quality, 4 = better than expected or needed diagnostic quality).

The severity of artifacts was graded separately for monoenergetic and MDI images on 3-point scale (1 = No artifacts; 2 = minimal artifacts with no effect on diagnostic interpretation; 3 = artifacts with substantial effect on diagnostic confidence- diagnosis not possible).

MDI images for each DECT exam were separately assessed for perfusion defects in the lungs. Abnormal lung perfusion was categorized into matched (low perfusion areas on MDI images match with the areas of low attenuation on monoenergetic images) and mismatched (low perfusion areas on MDI images do not have matching low attenuation on the monoenergetic images) defects [4]. When present, heterogeneity in lung perfusion on MDI images was graded (1 = expected, 2 = mild

artifactual heterogeneity, 3= marked artifactual heterogeneity).

Expected perfusion included homogenous (with no anteroposterior or apicobasal perfusion variations), physiologic perfusion (with greater iodine perfusion in the dependent regions and bases), or matched and mismatched perfusion defects described above. Artifactual heterogeneity was defined as a perfusion "abnormality" in the lungs which was neither expected perfusion nor represented any clear cut matched or mismatched defect). When confined to a part or a lobe of the lung, it was termed minimal; multilobar or diffuse artifactual heterogeneity in perfusion was termed as marked.

2.4. Quantitative assessment and radiation doses

In each transverse monoenergetic images (194 series), two study coinvestigators (SR and FH) recorded CT attenuation numbers (Hounsfield Units) and standard deviation (image noise) within the main pulmonary trunk by drawing a single circular region of interest (occupying 2/3rd of the lumen) on PACS workstation. Image sections and areas with contrast streaking were avoided when drawing the regions of interest.

Patient demographics, size specific dose estimates (SSDE), effective diameter, and water equivalent diameter (WED) for each DECT examination were obtained from a commercial CT radiation dose tracking and monitoring software (Radimetrics Enterprise Platform, Bayer Healthcare Medical Care, Whippany, NJ). The effective diameter refers to the square root of the product of anterior-posterior and lateral diameters of the patient. The WED refers to the diameter of a cylindrical water volume with average attenuation equivalent to the patient [9–14]. It is a patient size metric recommended by the American Association of Physicists in Medicine, and estimated automatically by our dose monitoring software [15].

2.5. Statistical analysis

Data were recorded and analyzed in Microsoft EXCEL (Microsoft Inc., Redmond, Wash.). Two-tail Student's *t*-test was used to compare the dose descriptors (SSDE), patient size (weight, WED), and Hounsfield units for DECT examinations. Mean and standard deviation were calculated for each quantitative metric. Wilcoxon signed rank and Cohen's κ tests were performed to compare and to assess interobserver agreement for qualitative evaluation of the DECT examinations. A p-value of ≤ 0.05 was considered statistically significant. For Cohen's Kappa analysis, a value of > 0.6 was deemed statistically significant.

3. Results

3.1. Quantitative assessment

The mean (± standard error of mean) for patient weight were not significantly different between the two DECT scanners (p = 0.88). SSDE (median and interquartile range) summarized in Table 1 were also comparable between the two scanners (p = 0.06). Information pertaining to the HU and image noise are summarized in Table 1.

Table 1
Quantitative parameters for SS-DECT and DS-DECT examinations. HU number and noise for main pulmonary artery (MPA) and radiation dose parameters. The water equivalent diameter refers to the diameter of a cylindrical water volume with average attenuation equivalent to the patient. Values are in mean (standard error of mean) for attenuation values and noise, mean (range) for patient weight and median (interquartile range) for radiation dose parameters.

	Patient Weight (kg)	Water equivalent diameter (WED)	HU	Noise	SSDE (mGy)
SS-DECT	72 (17)	280 (259-297)	366 (159)	20 (9)	8 (7-10)
DS-DECT	73 (18)	265 (243-284)	405 (139)	14 (5)	8 (7-9)
P-value	0.88	0.002	0.06	< 0.0001	0.06

3.2. Monoenergetic 60 keV images

Detected findings included air trapping, emphysema, lung cysts, atelectasis, consolidation, lung masses, nodules, post-radiation fibrosis, mediastinal and/or hilar lymphadenopathy, thyroid nodules, cardiomegaly, pericardial effusion, coronary calcification and pleural effusions. No pulmonary emboli or pulmonary infarcts were seen on any CT exam. Both radiologists reported minimal artifacts in 71/97 (73%) of SS-DECT and 58/97 (60%) of DS-DECT exams (p = 0.4-0.8) (Fig. 1). No artifacts were reported in the remaining 26/97 (27%) and 39/97 (40%) exams performed with the SS-DECT and DS-DECT techniques, respectively (p = 0.4-0.8). There was substantial interobserver agreement between the two radiologists for evaluation of artifacts on monoenergetic images (kappa = 0.72-0.76). Artifacts included contrast streaking, cardiac pulsation artifacts, streaking from pacemakers and wires, and beam hardening at the level of the shoulders. None of the artifacts were deemed severe or had any effect on diagnostic confidence. Diagnostic quality was deemed excellent for both DECT techniques.

3.3. MDI images

No mismatched perfusion defects suggested of pulmonary embolism or vascular abnormality were seen in any of the included DECT examinations. All abnormal perfusion defects on both scanners were matched defects with corresponding low attenuation region on the monoenergetic images. These corresponded areas of low attenuation regions related to air trapping, lung cysts, and emphysema. Both radiologists reported artifactual heterogeneities in perfusion (Fig. 2) on most SS-DECT MDI images (Table 2). These heterogeneities were marked and compromised evaluation of lung perfusion in 65% (63/97) of SS-DECT MDI images for one radiologist and 73%(71/97) of SS-DECT MDI images for the other radiologist (kappa co-efficient = 0.69). No artifactual heterogeneity was seen on the DS-DECT MDI images by either radiologist (Fig. 3) in contradistinction to the SS-DECT (p < 0.0001). Most beam hardening artifacts (> 50%) on both scanners were related to contrast streaking from subclavian veins and were categorized as minimal (p = 0.42-0.56). Remaining artifacts included streaking from pacemaker devices and ECG wires.

4. Discussion

Despite identical patients and associated radiation doses, there were substantial differences in material decomposition iodine images generated from SS-DECT and DS-DECT techniques. Both radiologists reported frequent artifactual heterogeneity without attributable pulmonary or vascular causes on MDI images from SS-DECT (in 63-71/97 patients) which was marked in 2/3 of exams, and confounded evaluation of pulmonary perfusion. Although cause for such artifactual heterogeneity is not known, a recent case report also presented similar image appearance on the MDI images from SS-DECT technique [16]. Furthermore, the report also found abnormal heterogeneity of lungs on MDI images of a patient who underwent a non-contrast SS-DECT [16]. This supports the fact that the perfusion heterogeneity on the MDI images was indeed artifactual and likely related to image processing or reconstruction issues rather than abnormalities in pulmonary perfusion. The artifactual nature of the heterogenous perfusion on MDI images from rapid kV technique is further supported by the fact that there were no pulmonary vascular abnormalities or airway related changes in pulmonary parenchymal attenuation (such as those from air trapping) on monoenergetic images from either technique, and there was presence of homogeneous perfusion distribution in MDI images of the same patients scanned with dual-source DECT technique. The artifactual heterogeneity tend to have a patchy and heterogenous distribution which does not correspond to any vascular territory. However, the

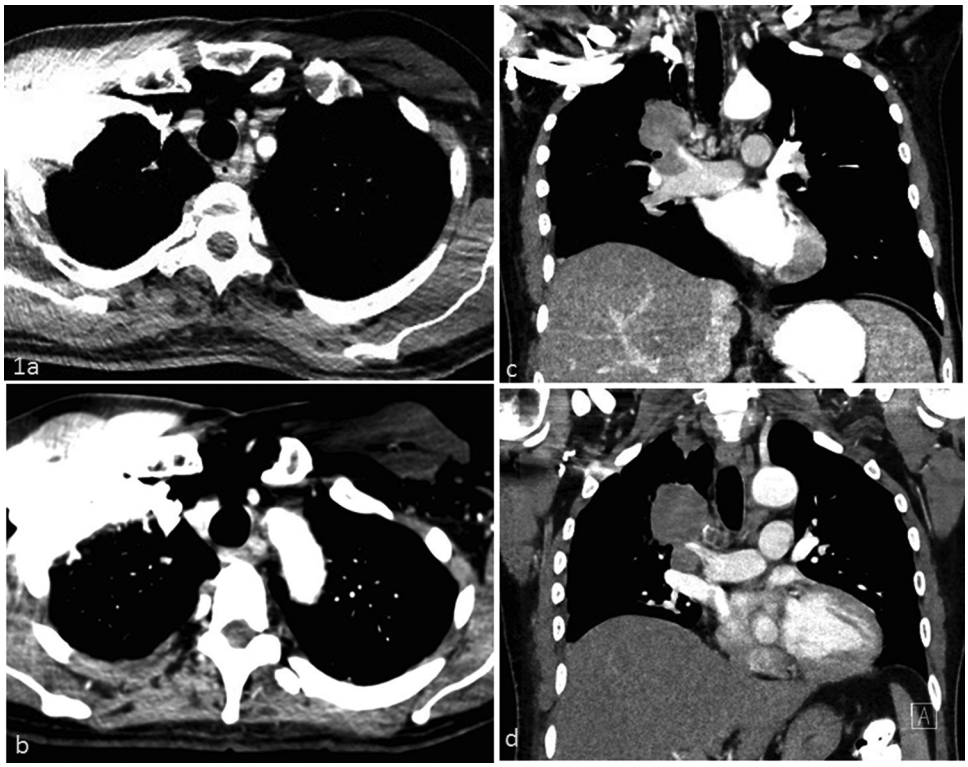

Fig. 1. Transverse, monoenergetic 60 keV images of a 58-year-old man (84 kg) scanned with SS-DECT (a) and DS-DECT (b) techniques demonstrate beam hardening artifacts due to intravenous contrast agent in the right subclavian vein. Monoenergetic 60 KeV coronal images from SS-DECT (c) and DS-DECT (d) techniques show a right hilar mass.

pattern can be confused with other perfusion abnormalities such as air trapping or chronic pulmonary thromboembolic diseases.

The presence of such pulmonary heterogeneity on the non-contrast MDI images in addition to the post-contrast MDI images raises possibility of suboptimal or erroneous material decomposition on SS-DECT. Although contrast streaking artifacts lead to pulmonary perfusion defects, these can be differentiated based on the location and morphological appearance. Since processing of SS-DECT is performed in the projection data domain, the appearance may be related to image reconstruction issues or artifacts. Since the MDI pulmonary heterogeneity frequently leads to artifactual areas of low perfusion, it can confound interpretation of true pulmonary perfusion.

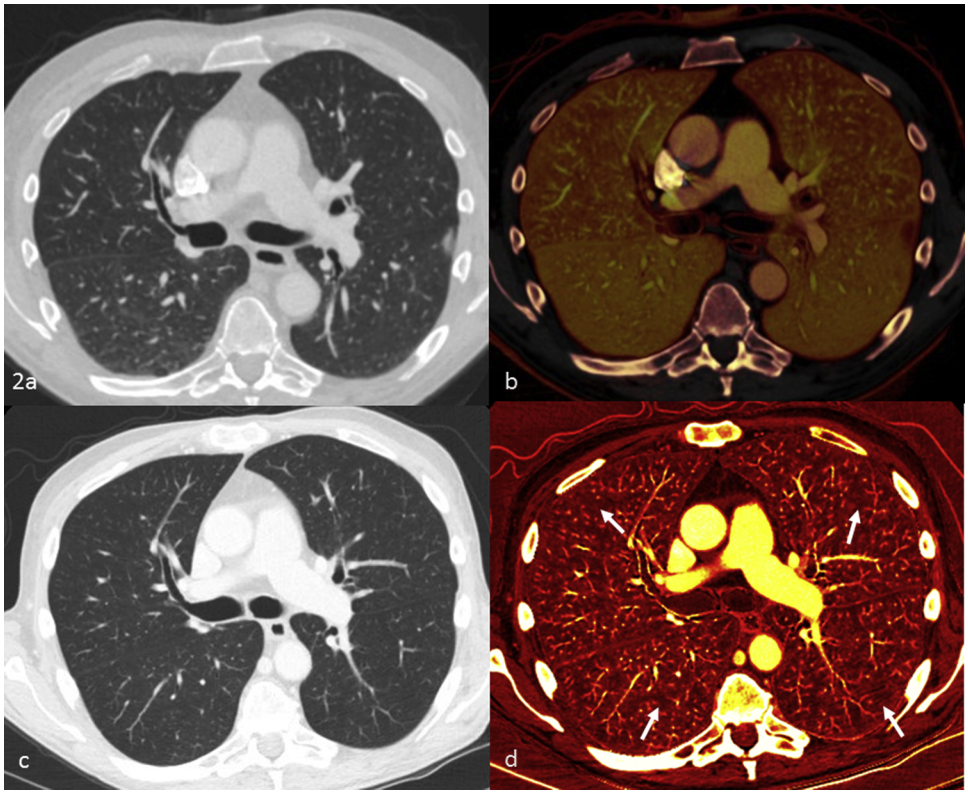

Fig. 2. A 63-year-old man (68 kg) underwent DS-DECT (a, b) and SS-DECT (c, d) for cancer surveillance. The transverse monoenergetic 60 KeV (a) image demonstrates a subpleural opacity in the left lower lobe which had resolved on the follow up monoenergetic 60 KeV (c) image. The transverse MDI image (b) from DS-DECT demonstrate gravity-based physiologic gradient in lung perfusion. The MDI image (d) from SS-DECT) are limited due to presence of artifactually heterogenous distribution of iodine in the lungs (white arrows).

Table 2
Distribution of artifactual heterogeneity of lung perfusion on SS-DECT and DS-DECT MDI images.

Artifactual heterogeneity	Radiologist 1		Radiologist 2	
	SS-DECT	DS-DECT	SS-DECT	DS-DECT
None	3	97	2	97
Minimal	31	0	24	0
Marked	63	0	71	0

We have alerted our radiologists about this artifactual appearance and the limited usability of MDI images from SS-DECT performed on the specific make and model of the scanner assessed in our study (GE Revolution CT). We have also informed the CT vendor about this artifactual or faulty image appearance on MDI images from this scanner. Users of SS-DECT can review the MDI images with the virtual monoenergetic images (in lung windows) to establish the artifactual perfusion heterogeneity in absence of parenchymal abnormality on monoenergetic images but such comparison will not work in presence of acute and chronic pulmonary embolism or pulmonary parenchymal abnormalities. In contrast to the SS-DECT MDI images, no artifactual heterogeneity in pulmonary perfusion was noted on DS-DECT MDI images. Such artifactual heterogeneity of MDI images has not been reported in prior studies with SS-DECT performed on GE Discovery 750 HD scanners [17,18]. In our practice, we have stopped using SS-DECT for any chest application on the Revolution CT although we continue to use SS-DECT on the Discovery 750 HD CT scanners without issues. Although causes of its selective presence was not assessed in our study, these artifacts may have stemmed from issues related to differences in the scanner hardware (such as 8 cm vs. 4 cm detector width for DECT), image reconstruction (ASiRv vs. ASiR iterative reconstruction technique), or DECT post-processing techniques between the Revolution and the Discovery 750 HD CT scanners.

Both radiologists found no or minimal artifacts on the virtual monoenergetic images generated from either SS-DECT or DS-DECT techniques. There were no differences between abnormalities seen on virtual monoenergetic images of each patient's DS-DECT and SS-DECT examinations. Diagnostic quality of virtual monoenergetic images was deemed excellent for all DECT examinations. There was no significant statistical difference in the CT attenuation number in the monoenergetic image series from either vendor ($p > 0.05$). The objective image noise on monoenergetic images from the two scanners was statistically significantly different ($p < 0.0001$). Also, despite differences in acquisition techniques between the two DECT scanners in terms of automatic exposure control, SSDE associated with DS-DECT and SS-DECT examinations were similar.

The main implication of our study lies in the fact that there are substantial differences in appearance of material decomposition images obtained from SS-DECT and DS-DECT scanners. Users should exercise caution when interpreting MDI images from SS-DECT due to artifactual heterogeneity in pulmonary perfusion. The artifactual heterogeneity can obscure evaluation in patients with chronic pulmonary thromboembolic pulmonary hypertension who have subsegmental or atypical pulmonary perfusion defects on MDI images [19].

Although we did not find a substantial difference in radiation doses associated with the two techniques, the DS-DECT allows automatic exposure control technique, and thus better adjustment of radiation dose versus fixed tube current scanning with the SS-DECT. Likewise, the availability of different kV pairs with the DS-DECT technique (from 70/150 to 100–150 kV) offers greater flexibility to adapt radiation doses to different patient sizes as opposed to a single 80/140 kV setting available with the SS-DECT technique. The radiation doses noted in our study were like those reported in the prior studies [3,20,21]. Canellas et al. have reported SSDE of 7.0 ± 1.2 mGy for standard of care chest DECT examination with the second-generation, 128-slice dual source CT (Somatom Flash, Siemens Healthineers) [3,20]. Our doses were also similar to those reported for DECT pulmonary angiography on the first- and second-generation, dual source CT [21]. Renapurkar et al have reported mean SSDE of 8.4 ± 1.2 mGy with use of 80/140 kV pair for DS-DECT pulmonary angiography which is also identical to the median SSDE of 8 mGy in our study [22].

Our study has limitations. Due to inherent differences in image appearance (gray scale from SS-DECT and colored images from DS-DECT), it was not possible to perform a blinded evaluation. Although it is possible to convert the gray-scale SS-DECT images to colored images, however, the resulted colors apply across the entire imaged anatomy and is not confined to lungs only as is the case for DS-DECT images due to the unique initial lung segmentation step applied on the DS-DECT software. However, none of the authors had any conflict of interest with

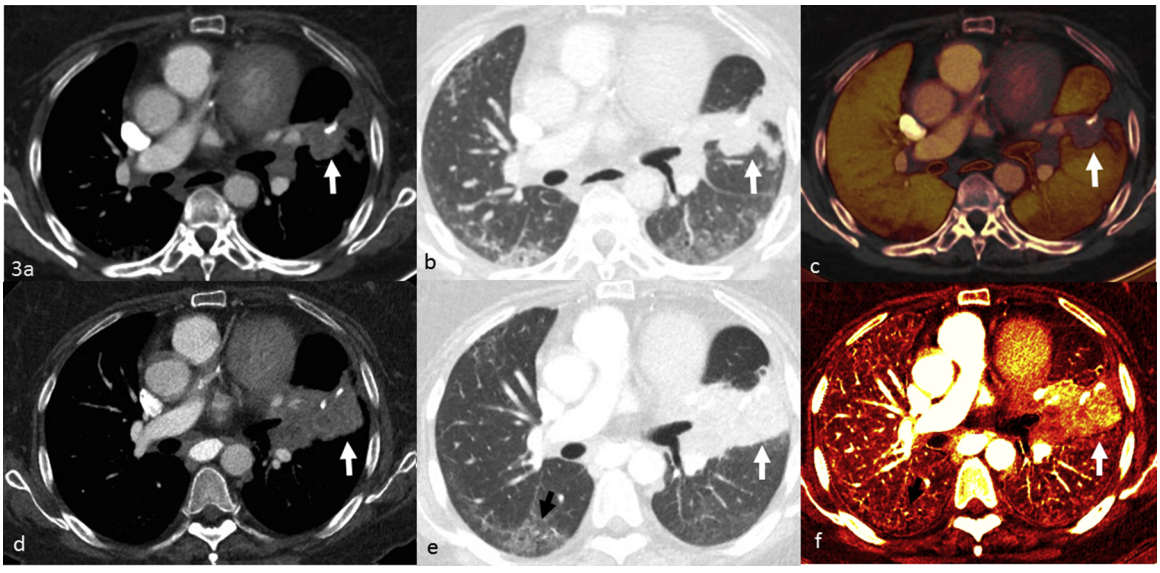

Fig. 3. A 53-year-old woman (72 kg) with lung cancer underwent DS-DECT (a) and follow-up SS-DECT (d) examinations at 3-month interval. A lingular mass (white arrow) is noted on all images. DS-DECT MDI image (c) show decreased perfusion in the lung bases corresponding to the area of pulmonary opacities seen on the DS-DECT monoenergetic (b) and SS-DECT monoenergetic (e) images. However, artifactual heterogeneity on SS-DECT MDI image (f) masks the expected abnormal perfusion (black arrows).

either vendor, and performed a fair, unbiased evaluation. We did not perform power analysis since this was a retrospective study of DECT examinations acquired for clinically indicated reasons. We included all eligible patients who underwent SS-DECT and DS-DECT. However, it was not feasible to scan the patients at the same time on both scanners. Although a larger study sample size was possible, it would have implied inclusion of separate patients or different CT scanning or injection protocols for the two DECT techniques. Although there were no substantial changes in abnormalities over the two DECT examinations performed in each patient, a subtle change in findings over the two examinations could have affected subjective evaluation of the images. Our results are also limited to the current operating versions of the two assessed CT scanners and do not apply to other scanners from the same or different vendors.

In summary, our study demonstrates that radiation doses and monoenergetic images from rapid kV-switching and dual source based DECT of the chest are similar but there are considerable variations in appearance of material decomposition-iodine images acquired with these two techniques. Radiologists must know the limitations of material decomposition iodine images acquired with rapid kV-switching when interpreting pulmonary perfusion defects.

Declaration of Competing Interest

The authors state that this work has not received any funding. The scientific guarantor of this publication is Subba R Digumarthy. The authors of this manuscript declare no relationships with any companies, whose products or services may be related to the subject matter of the article. No complex statistical methods were necessary for this paper. Written informed consent was waived by the Institutional Review Board. Institutional Review Board approval was obtained. The methodology of this study is observational study. None of the co-authors had any conflict of interest associated with this work.

References

[1] M.J. Sangwaiya, M.K. Kalra, A. Sharma, E.F. Halpern, J.A. Shepard, S.R. Digumarthy, Dual-energy computed tomographic pulmonary angiography: a pilot study to assess the effect on image quality and diagnostic confidence, J. Comput. Assist. Tomogr. 34 (January (1)) (2010) 46–51.

[2] S. McDermott, A. Otrakji, E.J. Flores, M.K. Kalra, J.O. Shepard, S.R. Digumarthy, Should dual-energy computed tomography pulmonary angiography replace single-energy computed tomography pulmonary angiography in pregnant and postpartum patients? J. Comput. Assist. Tomogr. 42 (January/February (1)) (2018) 25–32.

[3] R. Canellas, J.B. Ackman, S.R. Digumarthy, et al., Submillisievert chest dual energy computed tomography: a pilot study, Br. J. Radiol. 91 (1082) (2018) 20170735.

[4] A. Otrakji, S.R. Digumarthy, R. Lo Gullo, E.J. Flores, J.A. Shepard, M.K. Kalra, C.T. Dual-Energy, Spectrum of thoracic abnormalities, Radiographics 36 (January-February (1)) (2016) 38–52.

[5] J.B. Solomon, O. Christianson, E. Samei, Quantitative comparison of noise texture across CT scanners from different manufacturers, Med. Phys. 39 (10) (2012) 6048–6055.

[6] A.E. Papadakis, J. Damilakis, Fast kVp-switching dual energy contrast-enhanced thorax and cardiac CT: a phantom study on the accuracy of iodine concentration and effective atomic number measurement, Med. Phys. 44 (9) (2017) 4724–4735.

[7] R. Wu, Y. Watanabe, K. Satoh, et al., Quantitative comparison of virtual monochromatic images of dual energy computed tomography systems: beam hardening artifact correction and variance in computed tomography numbers: a phantom study, J. Comput. Assist. Tomogr. 42 (4) (2018) 648–654.

[8] R.W. van Hamersvelt, N.G. Eijsvoogel, C. Mihl, et al., Contrast agent concentration optimization in CTA using low tube voltage and dual-energy CT in multiple vendors: a phantom study, Int. J. Cardiovasc. Imaging 34 (8) (2018) 1265–1275.

[9] A. Daudelin, D. Medich, S.Y. Andrabi, C. Martel, Comparison of methods to estimate water-equivalent diameter for calculation of patient dose, J. Appl. Clin. Med. Phys. 19 (September (5)) (2018) 718–723.

[10] W. Huda, E.M. Scalzetti, M. Roskopf, Effective doses to patients undergoing thoracic computed tomography examinations, Med. Phys. 27 (2000) 838–844.

[11] J. Menke, Comparison of different body size parameters for individual dose adaptation in body CT of adults, Radiology 236 (2005) 565–571.

[12] T. Toth, Z. Ge, M.P. Daly, The influence of patient centering on CT dose and image noise, Med. Phys. 34 (2007) 3093–3101.

[13] J. Wang, J.A. Christner, X. Duan, S. Leng, L. Yu, C.H. McCollough, Attenuation-based determination of patient size for the purpose of size specific dose estimation in CT: part II. Implementation on abdomen and thorax phantoms using cross sectional CT images and scanned projection tadiograph images, Med. Phys. 39 (2012) 6772.

[14] J. Wang, X. Duan, J.A. Christner, S. Leng, L. Yu, C.H. McCollough, Attenuation-based estimation of patient size for the purpose of size specific dose estimation in CT. Part I. Development and validation of methods using the CT image, Med. Phys. 39 (2012) 6764.

[15] C. McCollough, D.M. Bakalyar, M. Bostani, et al., Use of water equivalent diameter for calculating patient size and size-specific dose estimates (SSDE) in CT: the report of AAPM task group 220, AAPM Rep. 2014 (2014) 6–23.

[16] R. Borse, F. Homayounieh, R. Singh, S.R. Digumarthy, Heterogeneous pulmonary perfusion on dual-energy computed tomography: faulty postprocessing or new artifact? J. Comput. Assist. Tomogr. 42 (November/December (6)) (2018) 885–886.

[17] X.R. Cai, Y.Z. Feng, L. Qiu, Z.H. Xian, W.C. Yang, X.K. Mo, X.B. Wang, Iodine distribution map in dual-energy computed tomography pulmonary artery imaging with rapid kVp switching for the diagnostic analysis and quantitative evaluation of acute pulmonary embolism, Acad. Radiol. 22 (June (6)) (2015) 743–751.

[18] L.L. Geyer, M. Scherr, M. Körner, S. Wirth, P. Deak, M.F. Reiser, U. Linsenmaier, Imaging of acute pulmonary embolism using a dual energy CT system with rapid kVp switching: initial results, Eur. J. Radiol. 81 (December (12)) (2012) 3711–3718.

[19] G. Dournes, D. Verdier, M. Montaudon, et al., Dual-energy CT perfusion and angiography in chronic thromboembolic pulmonary hypertension: diagnostic accuracy and concordance with radionuclide scintigraphy, Eur. Radiol. 24 (1) (2014) 42–51.

[20] R. Canellas, S. Digumarthy, A. Tabari, et al., Radiation dose reduction in chest dual-energy computed tomography: effect on image quality and diagnostic information, Radiol. Bras. 51 (6) (2018) 377–384.

[21] R.W. Bauer, S. Kramer, M. Renker, et al., Dose and image quality at CT pulmonary angiography-comparison of first and second generation dual-energy CT and 64-slice CT, Eur. Radiol. 21 (10) (2011) 2139–2147.

[22] R.D. Renapurkar, A. Primak, J. Azok, et al., Attenuation-based kV pair selection in dual source dual energy computed tomography angiography of the chest: impact on radiation dose and image quality, Eur. Radiol. 27 (8) (2017) 3283–3289.